

Dynamic Ventilation Scintigraphy: A Comparison of Parameter Estimation Gating Models

Stanley N. Hack, Robert A. Paoni, Howard Stratton, Marigrace Valvano, Bruce R. Line, and Jeffrey A. Cooper

TAU Corporation, Los Gatos, California; XRE Corporation, Littleton, Massachusetts; The State University of New York, Albany, New York; and Albany Medical College, Albany, New York

Two procedures for providing the synchronization of ventilation scintigraphic data to create dynamic displays of the pulmonary cycle are described and compared. These techniques are based on estimating instantaneous lung volume by pneumotachometry and by scintigraphy. Twenty-three patients were studied by these two techniques. The results indicate that the estimation of the times of end-inspiration and end-expiration are equivalent by the two techniques but the morphologies of the two estimated time-volume waveforms are not equivalent. Ventilation cinescintigraphy based on time division gating but not on isovolume division gating can be equivalently generated from list mode acquired data by employing either technique described.

J Nucl Med 29:1842-1847, 1988

It has been suggested that dynamically gated pulmonary ventilation scintigraphy can provide added clinical information regarding the state of the respiratory system as compared to static, time averaged studies (1). The display of this information can take the form of a cine loop derived from a multi-cycle pulmonary-gated acquisition of the lungs while the patient breathes air labeled with a radioactive inert gas. Several methods of implementing the required pulmonary-gating based on parameter estimation of the dynamic lung volume and, in some cases, airway flow have been studied. These techniques are based on estimating the dynamic lung volume by means of spirometry, pneumotachometry (2), or impedance plethysmography (3) in addition to estimating the dynamic lung volume scintigraphically by integrating gamma events detected over the lung field while the patient breathes a radiolabeled gas (1).

In this present study, we compare the estimations of instantaneous lung volume based on pneumotachometry versus direct integration of gamma events detected over the lung field during a scintigraphic ventilation

study. Pneumotachometry derived volume signals are obtained by time-integrating the flow signal output of a pneumotachometer through which a patient breathes during a scintigraphic ventilation study. The scintigraphically derived volume signal is obtained by spatially integrating the gamma events detected over the lung field during discrete time intervals followed by temporally filtering the resulting signals. We compare the resulting times of end-expiration and end-inspiration as obtained by both methods. In addition, we compare the morphology of the time-volume signals as estimated by both methods. The goal of the study is to determine if time division or isovolume division gating of ventilation cinescintigraphy can be equivalently generated using pneumotachometry and scintigraphy based techniques.

METHODS

Twenty-three patients were studied using standard xenon-133 (^{133}Xe) ventilation scintigraphic techniques (4) with the addition of a pneumotachometer placed in the breathing circuit. The patients rebreathed a mixture of 15 mCi of ^{133}Xe in 8 l of oxygen in a closed system for a period of 5 min. The breathing circuit was then open to the atmosphere for the washout phase of the study, which lasted from 0.5 to 10 min.

Received May 18, 1987; revision accepted July 7, 1988.
For reprints contact: Stanley N. Hack, BSC, TAU Corporation,
485 Alberto Lane, Building D, Los Gatos, CA 95032.

List mode scintigraphic data were merged in a temporal fashion with the airway flow data obtained at 10-msec intervals from the pneumotachometer. Postprocessing analysis of the pneumotachometer derived airway parameters were compared to the airway parameters estimated directly from the scintigraphic data. A flowchart of the processing and analysis is shown in Figure 1.

Pneumotachometer Data Processing

As shown in Figure 1, the pneumotachometer airway flow data as sampled at 10 msec intervals are integrated temporally and resampled at 10 samples/sec (100 msec intervals) to provide computed airway volume data as a function of time (Step P-1). End-inspiration and end-expiration times are found from the volume data by locating local minima and maxima of the volume signal (Step P-2). To maximize noise tolerance, the algorithm used to detect local minima and maxima is based on locating sign changes in the average slope of one second segments of the volume data. The average slope computations use least square error fits of straight lines to one second segments of the volume signal waveform. Each subsequent slope calculation includes the last 0.9 sec of data used in the previous slope computation in addition to the next sampled point of the volume signal. Next, the volume signal is normalized using a mean/s.d. normalization technique as (Step P-3).

$$VOL(t) = (VOL(t) - MEAN) / STANDARD DEVIATION. \quad (1)$$

The mean and s.d. used in Eq. (1) are computed from the entire volume signal. Finally, the volume signal is normalized on a cycle-by-cycle basis (Step P-4). Each signal segment bounded by a minima or maxima on either side is normalized according to the amplitude difference between the minima point and the maxima point as

$$VOL(t) = (VOL(t) - VOL(min)) / (VOL(max) - VOL(min)). \quad (2)$$

Note that this cycle-by-cycle normalizing technique assigns an amplitude of 0.0 to all minima and assigns an amplitude of 1.0 to all maxima.

Admittedly, mean/s.d. normalization and cycle-by-cycle normalization are redundant. Both techniques were used in order to compare the morphologies of the flow signal and the scintigraphy signal following an easily implemented normalization process (the former) and a more involved normalization process (the latter).

Scintigraphic Data Processing

As shown in Figure 1, the ^{133}Xe ventilation data are segmented into 100-msec frames in which the data are summed both temporally and spatially to yield a counts versus time signal (Step S-1). Low count frames in the beginning and end of the study are eliminated due to their poor signal-to-noise ratio in Step S-2 of Figure 1. The criteria used is to truncate the head and tail of the study so that the minimum counts/100 msec frame never falls below 10% of the that of the frame containing the maximum number of counts over the entire study. The counts versus time signal is then low pass filtered with a cutoff frequency of 0.6 Hz using a finite impulse response (FIR) digital filter (Step S-3) (5). This step eliminates

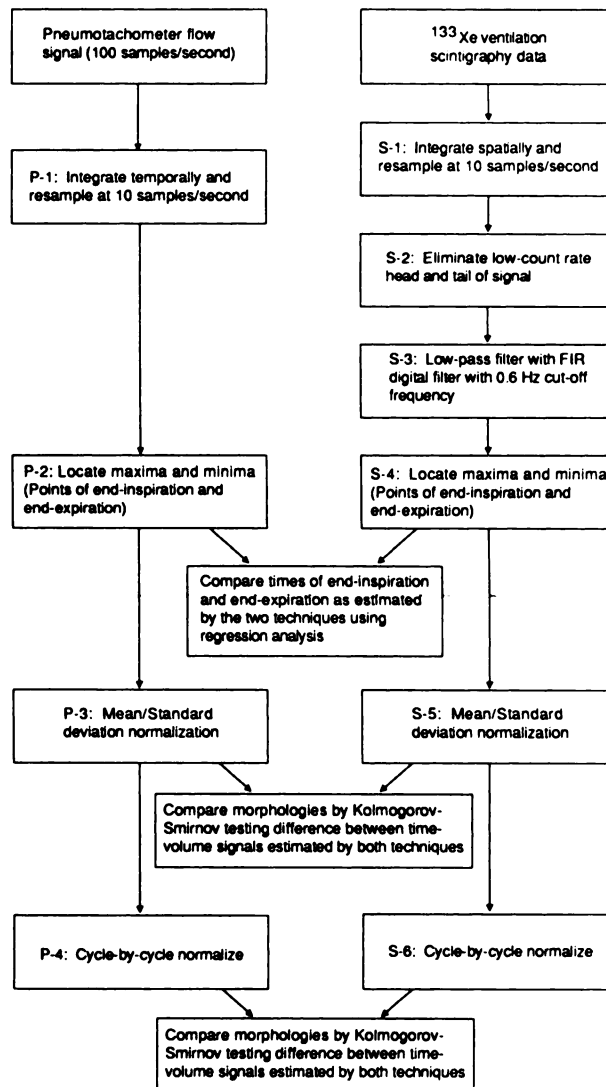


FIGURE 1 Flowchart of processing and analysis of respiratory time-volume waveforms estimated from pneumotachometry and scintigraphy.

much of the high frequency noise which is imposed on the signal due to poor counting statistics. Times of end-inspiration and end-expiration are located by finding all local minima and maxima as described in Step P-2 above (Step S-4). The final two steps of the post-processing of the scintigraphic data are described in Steps P-3 and P-4 above. These steps are signal normalization by mean and standard deviation as per Eq. (1) (Step S-5), and cycle-by-cycle normalization as per Eq. (2) (Step S-6).

Signal Comparisons

The airway flow versus time signal estimated from pneumotachometry and the counts versus time signal derived from the scintigraphic data are compared following three different stages of signal postprocessing. The first comparison analyzes the estimated times of end-inspiration and end-expiration as determined from both signals. This comparison is performed following Steps P-2 and P-4 above by regression analysis of the function of end-inspiration times and end-expiration times

estimated by the scintigraphic method versus the end-inspiration and end-expiration times as estimated by pneumotachometry. The second and third analysis compare the morphology of the pneumotachometry derived signal and the scintigraphy derived signal at two stages of the postprocessing. The second analysis compares the morphology of the signals following normalization by the mean and s.d. method (Steps P-3 and S-5 above) as per Eq. (1). The third analysis compares the morphology of the signals following cycle-by-cycle normalization (Steps P-4 and S-6 above) according to Eq. (2). The third comparison is performed to ascertain the effects of additional signal processing in the form of cycle-by-cycle normalization. These comparisons are based on the null hypothesis that the difference between the two signals is white noise. To test this null hypothesis, the difference between the two signals in question is calculated. This difference is Fourier transformed to produce a power spectrum or a periodogram. The resulting periodogram is compared to a periodogram of amplitude zero at all frequencies using the Kolmogorov-Smirnov goodness-of-fit test (6). The null hypothesis is then accepted or rejected at the 99%, 95%, 90%, and 80% confidence levels.

RESULTS

A total of 23 patient studies including an aggregate of 12,511 sec of data collection and a total of 2,082 pulmonary cycles were evaluated. The goal in selecting the amount of data required for this study was to minimize the impact of individual anomalous pulmonary cycles on the total results but to permit abnormal patient studies to stand out. Accordingly, we selected a data set containing greater than 2,000 pulmonary cycles so that each individual cycle will have an impact of

only 0.05% on the results of the entire study. This data set includes 23 patient studies, however, so that each patient study will have an impact of nearly 5% on the overall study.

Figure 2 illustrates the results of the signal postprocessing applied to the pneumotachometer derived data. Figure 2A is an example of a 51-sec segment of the pneumotachometer derived signal following temporal integration and 100-msec resampling (Step P-1) and mean/standard deviation normalization (Step P-3). Figure 2B shows the same signal segment following cycle-by-cycle normalization (Step P-4).

Figure 3 illustrates the results of the signal postprocessing applied to the scintigraphically derived volume signal. Figure 3A is an example of a 51-sec segment of the integrated count data representing instantaneous pulmonary volume (Step S-1). The same segment following FIR low-pass filtering with a cutoff frequency of 0.6 Hz (Step S-3) and mean/standard deviation normalization (Step S-4) is shown in Figure 3B. Figure 3C shows the same signal segment following cycle-by-cycle normalization (Step S-5). Note that the data segments shown in Figure 3 have a direct time correspondence with the data segments depicted in Figure 2.

The estimates of end-inspiration and end-expiration times as determined by pneumotachometry and scintigraphy compare favorably. Table 1 lists the mean \pm s.d. corresponding pulmonary cycle lengths for each patient study as determined by scintigraphy and pneumotachometry. In addition, the RMS error between pulmonary cycle times as determined by both techniques on a breath-by-breath basis for each patient study is shown in the table. The square of the differences of pulmonary

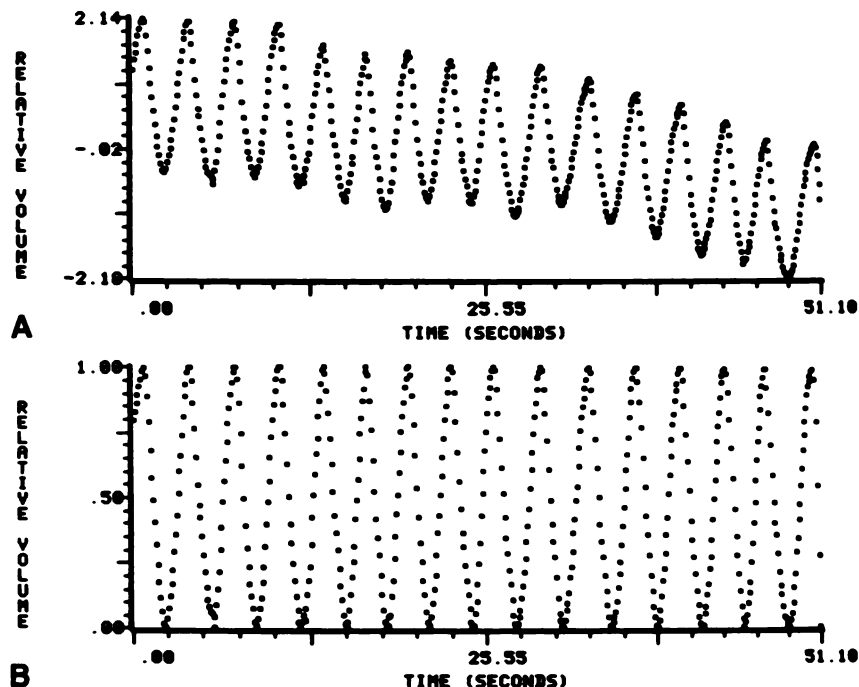


FIGURE 2
Results of signal processing a 51-sec sample of the pneumotachometry based time-volume waveform. A: Volume signal computed by temporal integration of pneumotachometer flow signal and resampled with a period of 100 msec followed by mean/standard deviation normalization as per Eq. (1). B: Normalized volume data following cycle-by-cycle normalization as per Eq. (2).

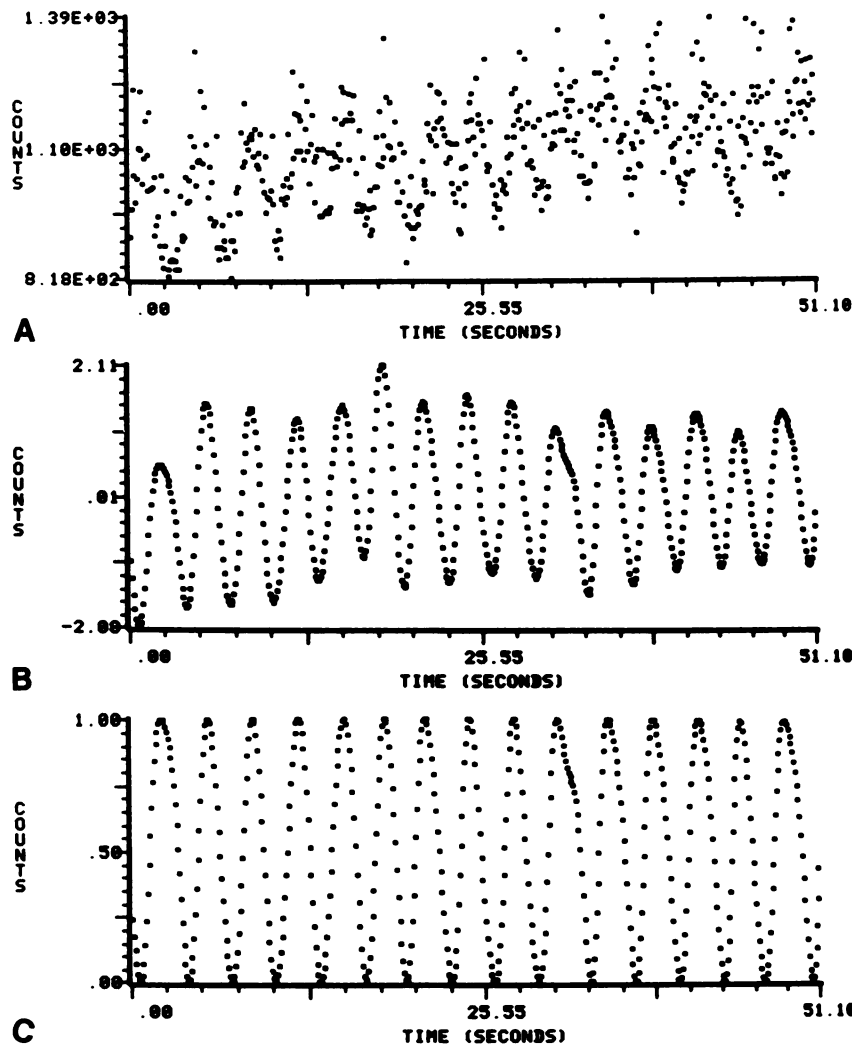


FIGURE 3
Results of signal processing a 51-sec sample of the scintigraphy based time-volume waveform. A: Temporally and spatially integrated gamma count data to estimate the relative instantaneous pulmonary time-volume signal. B: Scintigraphically estimated volume signal following FIR low-pass filtering with a cutoff frequency of 0.6 Hz followed by mean/standard deviation normalization as per Eq. (1). C: Filtered volume data following cycle-by-cycle normalization as per Eq. (2).

cycle times between corresponding pulmonary cycles as derived by the two techniques are summed for an entire patient study. The square root of this summation is divided by the number of pulmonary cycles studied and is expressed as a percentage of the mean cycle time of the study computed by the two techniques. The RMS error is given by Eq. (3) as follows:

$$\text{RMS} = \frac{\sqrt{\sum_{i=1}^N (T_{pi} - T_{si})^2 / N}}{\frac{1}{2} (\bar{T}_p - \bar{T}_s)}, \quad (3)$$

where

- N = number of pulmonary cycles in the study;
- T_{pi} = pulmonary cycle period as computed by pneumotachometry for pulmonary cycle i ;
- T_{si} = pulmonary cycle period as computed by scintigraphy for pulmonary cycle i ;
- \bar{T}_p = mean period of pulmonary cycles as computed by pneumotachometry;
- \bar{T}_s = mean period of pulmonary cycles as computed by scintigraphy.

With one exception, the RMS cycle time errors do not exceed 5% of the mean pulmonary cycle time. The RMS error of the single outlying data point is 28.5%. Furthermore, the mean percentage RMS error between corresponding pulmonary cycles (excluding the outlier) is 1.23% for the entire test data set.

The comparison of the pneumotachometer derived volume signal to the scintigraphically derived volume signal following mean/s.d. normalization and following cycle-by-cycle normalization yielded a rejection of the null hypothesis at all confidence levels selected. That is, based on the Kolmogorov-Smirnov goodness-of-fit test, we were unable to prove that the power spectrum of the difference between the two signals is attributable solely to white noise. Of course, both methods of normalization need not be applied to the data preceding comparison. However, it was our intention to compare the results of a relatively simple signal processing technique, namely, mean/s.d. normalization, to the results of a more complex technique, namely, cycle-by-cycle normalization. We found that volume signals from the

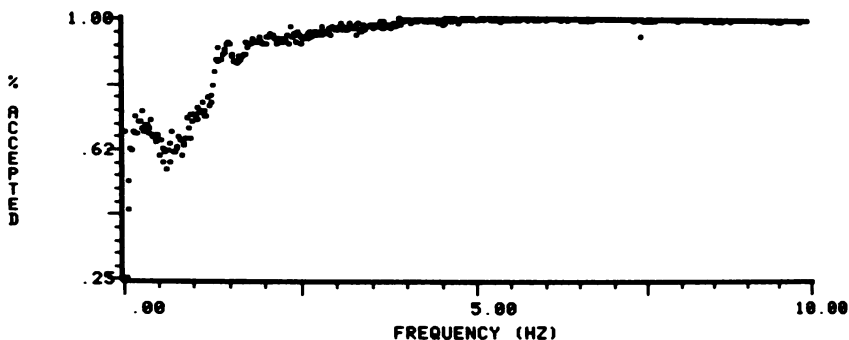
TABLE 1
Mean Pulmonary Cycle Times \pm s.d. (sec) as Determined by Scintigraphy and Pneumotachometry and Inter-Technique Cycle-by-Cycle Time RMS Errors Given as a Percentage of Mean Cycle Times

Patient no.	Study length (sec)	Scintigraphy	Pneumotachometry	RMS intertechnique error
		mean cycle time \pm s.d. (sec)	mean cycle time \pm s.d. (sec)	
1	350	4.87 \pm 1.15	4.80 \pm 0.91	1.52%
2	598	10.53 \pm 5.59	8.93 \pm 1.17	0.14%
3	649	8.58 \pm 5.81	7.17 \pm 1.72	1.13%
4	584	4.90 \pm 3.45	8.03 \pm 8.55	1.58%
5	774	6.71 \pm 5.40	5.10 \pm 0.69	0.58%
6	522	6.47 \pm 4.61	5.10 \pm 0.58	0.65%
7	331	4.99 \pm 0.97	5.36 \pm 1.11	2.12%
8	492	7.66 \pm 5.24	6.21 \pm 0.78	0.43%
9	788	6.17 \pm 4.48	4.85 \pm 0.75	0.70%
10	617	8.66 \pm 4.74	7.17 \pm 0.82	0.22%
11	398	8.51 \pm 2.92	8.06 \pm 1.41	3.21%
12	457	12.66 \pm 5.62	9.57 \pm 2.39	0.29%
13	598	6.76 \pm 4.44	5.24 \pm 0.62	0.70%
14	536	11.17 \pm 5.62	10.15 \pm 2.11	1.70%
15	492	11.49 \pm 4.05	11.43 \pm 2.64	0.78%
16	462	6.99 \pm 5.08	5.75 \pm 3.17	1.63%
17	515	10.00 \pm 7.58	6.67 \pm 0.96	0.41%
18	478	8.20 \pm 6.54	2.28 \pm 1.95	28.5%
19	312	6.60 \pm 2.60	6.25 \pm 0.72	2.21%
20	761	6.85 \pm 5.49	5.03 \pm 0.60	4.15%
21	807	9.57 \pm 5.71	8.26 \pm 1.58	1.80%
22	488	7.75 \pm 5.32	6.54 \pm 1.52	0.23%
23	502	6.21 \pm 4.74	5.76 \pm 2.43	0.97%

two sources did not compare favorably following either normalization technique.

Figure 4 shows a histogram of the fractional number of 51-sec segments of cycle-by-cycle normalized volume data determined by both techniques in which the null hypothesis was accepted at the 95% confidence level for each discrete frequency range investigated. The abscissa of this plot represents frequency quanta from 0.0 Hz to 10.0 Hz in 0.0196 Hz increments. The ordinate represents the number of 51-sec segments of patient studies for which the null hypothesis is accepted at a given frequency at the 95% confidence level. Note that the acceptance rate is very high at frequencies above

FIGURE 4
Histogram of the number of 51-sec data segments for each frequency range of the pneumotachometry estimated data and the scintigraphy estimated data which were accepted at the 95% confidence level by the Kolmogorov-Smirnov goodness-of-fit test as exhibiting equivalent morphologies. The abscissa represents frequency ranges from 0 Hz to 10 Hz. The ordinate represents the number of 51-sec segments of time-volume data as estimated by both techniques that were shown to be equivalent for each frequency range.



2.0 Hz. This shows that we were successful in removing the high frequency noise from the scintigraphy data, but the actual signals, as determined by scintigraphy and pneumotachometry, compare unfavorably even when sophisticated cycle-by-cycle normalization signal processing is used.

DISCUSSION

The signal processing described reduces noise, eliminates low frequency drift, and normalizes the volume signals as derived by both techniques in order to provide for artifact-free comparisons. Figure 3B shows an equivalent scintigraphy derived time-volume signal as that of Fig. 3A but with reduced high frequency noise. Mean/s.d. normalization removes signal inconsistencies that are due to the calibration and statistical nature of the acquisition methods and equipment used (Figs. 2A and 3B). Cycle-by-cycle normalization eliminates inter-signal variations including low frequency drift caused by temporal changes in the acquisition hardware and by temporal changes in the subject's breathing patterns. This latter form of normalization is valid for this study since any gating of pulmonary ventilation images is based on either relative timing or signal shape of each individual pulmonary cycle. In Figs. 2B and 3C we see the results of cycle-by-cycle normalization. Note that each pulmonary cycle in these two figures is equivalent in terms of total change in volume per cycle.

The results show that relative respiratory volumes as estimated by pneumotachometry and by ^{133}Xe ventilation scintigraphy yield equivalent pulmonary cycle timing based on analysis of frequency and phase. The volume signals estimated by the two techniques are usually out of phase, but this phase shift is constant throughout the entire study. However, even with extensive signal processing, the morphologies of the estimated volume signals are not equivalent. This latter observation is based on our inability to prove that the power spectrum of the difference between the two estimated volume signals is attributable solely to white noise by the Kolmogorov-Smirnov goodness-of-fit test

at confidence levels as low as 80%. From Figure 4 we see that the two volume signals are quite dissimilar at low frequencies, but they are similar, if not equivalent, at frequencies above ~ 2 Hz. This observation indicates that the signal processing eliminates high frequency noise above the 2 Hz frequency level in the scintigraphically based volume signal and that there is little or no noise in the pneumotachometry derived volume signal above 2 Hz. Furthermore, our results point out that the volume information of interest is at frequencies below 2 Hz.

In terms of producing equivalent recycling dynamic images of the breathing lung based on gated ventilation scintigraphy using scintigraphy or pneumotachometry based gating, our results indicate the following. The two techniques provide equivalent results if the segmentation of the pulmonary cycle is time-based as opposed to volume-based. That is, if the pulmonary gating results in image segments spanning a fixed fraction of time of each pulmonary cycle, then one only needs to determine the end-inspiration or end-expiration times in order to implement the gating. Our results show that equivalent end-inspiration and end-expiration times can be computed based on pneumotachometry or scintigraphy. The scintigraphic data used by this method need only be processed by spatial and temporal integration and by FIR filtering (Step S-1 through S-3 of Fig. 1). On the other hand, if segmentation of the pulmonary cycle is based on isovolumic segments each spanning a variable time-fraction of the pulmonary cycle, then gating based on the two techniques that we have studied is not equivalent even following relatively sophisticated signal processing operations including cycle-by-cycle normalization. It is beyond the scope of this study to determine which technique is more accurate, reliable, and repeatable if, in fact, one of these techniques exhibits an advantage over the other in these qualities.

Both Kaplan's group (1) and Line's group (2) base the segmenting of the pulmonary cycle in order to produce ventilation cinescintigrams only on the time-fractionation of each individual pulmonary cycle. Line derives the fiducial point times of the pulmonary cycle from pneumotachometry and Kaplan derives the timing data from scintigraphy. It is therefore our conclusion that these two techniques yield equivalent results. Note, however, that Line uses information derived from a plot of airway flow versus lung volume to exclude pulmonary cycles whose deviation from the norm exceeds a predetermined threshold. Heller's group (3) segments scintigrams based on isovolumic portions of the pulmonary cycle as derived from impedance plethysmography of the thorax. Our results indicate that equivalent gating of scintigrams by this technique would not yield equivalent results if the time-volume information were derived from either scintigraphy data or pneumotachometry data.

In summary, we have found that pulmonary cycle

gating of scintigraphic ventilation studies based on pneumotachometry and scintigraphically derived volume signals are equivalent when the gating is based solely on the time of occurrence of end-inspiration and end-expiration. However, for techniques in which pulmonary gating is dependent on the morphology of the time-volume signal, gating derived from pneumotachometry is not equivalent to gating derived from ventilation scintigraphy. Scintigraphically gated pulmonary ventilation studies can be acquired with standard nuclear medicine computing hardware which makes that technique relatively easy to implement in a clinical setting. However, physiological gating or dual isotope techniques must be employed for eliminating pulmonary motion artifacts from nonventilation scintigraphic studies.

Conversely, for gating techniques in which pulmonary gating is dependent upon the morphology of the time-volume signal, gating derived from pneumotachometry is not equivalent to gating derived from ventilation scintigraphy. One would assume pneumotachometry to be a more accurate indicator of lung volume. Pneumotachometry is, in fact however, a parameter estimation technique based on the measurement of differential pressures obtained from opposite sides of a partial airway obstruction. Accordingly, the determination of the most accurate parameter estimation technique for facilitating isovolume division pulmonary gating (i.e., scintigraphy based versus pneumotachometry based) would require a carefully planned and controlled study unto itself.

ACKNOWLEDGMENTS

The authors thank Ms. Susanne Freeman and Mr. Michael Ciarmiello for preparing the photographs and graphics used in this report and Ms. Janice Smith and Ms. Bobbie Fajardo for their expert preparation of this manuscript.

REFERENCES

1. Kaplan E, Gergans GA, Milo T, Friedman AM, Sharp JT. Dynamic imaging of the respiratory cycle with ^{81m}Kr . *Chest* 1982; 81:312-317.
2. Line BR, Cooper JA, Spicer KM, Jones AE, Crystal RG, Johnston GS. Radionuclide cinepneumography: flow-volume imaging of the respiratory cycle. *J Nucl Med* 1980; 21:219-224.
3. Heller SL, Scharf SC, Hardoff R, Blaurock MD. Cinematic display of respiratory organ motion with impedance techniques. *J Nucl Med* 1984; 25:1127-1131.
4. Markisz JA. Radiologic and nuclear medicine diagnosis. In: Goldhaber SZ, ed. *Pulmonary embolism and deep venous thrombosis*, Philadelphia: W. B. Saunders Company, 1985: 45-52.
5. Rabiner LR. Techniques for designing finite-duration impulse-response digital filters. *IEEE Trans Commun Technol* 1971; COM-19:188-195.
6. Allen AO. *Probability, statistics, and queuing theory with computer science applications*. Orlando, FL: Academic Press, 1978: 311-317.